Rieko Yamamoto
First *Last*

ASME Paper Title: Effectiveness of an Intelligent Foot Orthosis in Lateral Fall Prevention

Authors: Rieko Yamamoto, Sho Itami, Masashi Kawabata, Toshihiko Shiraishi

ASME Journal Title: The ASME Journal of Engineering and Science in Medical Diagnostics and Therapy (JESMDT)

Volume/Issue : Nov 2022, 5(4) Date of Publication (VOR* Online) : August 8, 2022

ASME Digital Collection URL: https://asmedigitalcollection.asme.org/medicaldiagnostics/article/5/4/041009/114331 of-an-Intelligent-Foot-Orthosis-in

DOI: https://doi.org/10.1115/1.4055040

*VOR (version of record)

ASME Journal of Engineering and Science in Medical Diagnostics and Therapy. Received February 28, 2022; Accepted manuscript posted July 22, 2022. doi:10.1115/1.4055040

Effectiveness of an Intelligent Foot Orthosis in Lateral Fall Prevention

Rieko YAMAMOTO*
Graduate School of Environment and Information Sciences, Yokohama National University
79-7, Tokiwadai, Hodogaya-ku, Yokohama, Kanagawa, 240-8501, Japan
Department of Rehabilitation Medicine, Keio University School of Medicine
35 Shinanomachi, Shinjuku, Tokyo, 160-8582, Japan
yama20rie@gmail.com

Sho ITAMI
Graduate School of Environment and Information Sciences, Yokohama National University
79-7, Tokiwadai, Hodogaya-ku, Yokohama, Kanagawa, 240-8501, Japan
itami-sho-ns@ynu.jp

Masashi KAWABATA
School of Allied Health Sciences, Kitasato University
1-15-1 Kitasato, Minami-ku, Sagamihara, Kanagawa 252-0373, Japan
mkawaba@kitasato-u.ac.jp

Toshihiko SHIRAISHI
Graduate School of Environment and Information Sciences, Yokohama National University
79-7, Tokiwadai, Hodogaya-ku, Yokohama, Kanagawa, 240-8501, Japan
shira@ynu.ac.jp
ASME Membership: #100226183

* Corresponding author:
Rieko YAMAMOTO *
Graduate School of Environment and Information Sciences, Yokohama National University *
79-7, Tokiwadai, Hodogaya-ku, Yokohama, Kanagawa, 240-8501, Japan
Department of Rehabilitation Medicine, Keio University School of Medicine
35 Shinanomachi, Shinjuku, Tokyo, 160-8582, Japan
yama20rie@gmail.com

ASME Journal of Engineering and Science in Medical Diagnostics and Therapy. Received February 28, 2022;
Accepted manuscript posted July 22, 2022. doi:10.1115/1.4055040

ABSTRACT

The aim of this study was to validate the effectiveness of the newly developed Intelligent Foot Orthosis (IFO) at preventing lateral falls. The IFO is a wearable fall prevention system based on using a small magnetorheological brake to control the height of the lateral sole. Experiments were performed to compare the walking motions on a lateral slope under four conditions: without IFO, with IFO current-OFF, with IFO current-ON, and with IFO control-ON. The mediolateral center of gravity and center of pressure horizontal distance (ML COG–COP HD) was measured in three-dimensional motion analysis to represent the change in posture on the frontal plane. To observe the corresponding muscular activity, surface electromyography (EMG) was performed to obtain the mean and peak root mean square (RMS) for the tibia anterior (TA) and peroneus longus (PL) in the first half of the stance phase when the IFO applied control. In the results, ML COG-COP HD increased significantly under the "with IFO control-ON" compared to the "without IFO" and "with IFO current-ON" conditions. The mean RMS of the TA was significantly decreased under the "with IFO current-ON" and "with IFO control-ON" conditions compared to the "without IFO" condition. These results demonstrate that the posture moved away from the lateral fall direction primarily due to IFO assistance rather than muscular activity, which would be a consequence of human postural control. Thus, the IFO does appear to help prevent lateral falls.
Keywords: Intelligent Foot Orthosis, fall prevention, lateral fall, gait control, magnetorheological (MR) fluid, 3D motion analysis, electromyography (EMG)

INTRODUCTION

For people with walking disabilities to live safely and independently, an important issue is to increase their range of independent mobility, which involves improving walking stability. In addition, fall prevention becomes an increasingly significant issue with age. Lateral falls are often associated with serious fractures leading to bedridden conditions. At least 1 in 3 community-dwelling elderly people fall each year,

ASME Journal of Engineering and Science in Medical Diagnostics and Therapy. Received February 28, 2022;
Accepted manuscript posted July 22, 2022. doi:10.1115/1.4055040

and 1 in 5 people who fall are seriously injured (1 in 10 suffer a fracture) and require long hospital stays [1]. In the United States, about 1 in 4 adults aged 65 and older experience a fall [2]. Among stroke patients, 73% experience a fall during the first 6 months after discharge [3]. More than 95% of hip fractures are caused by falls [4], which mainly comprise lateral falls [5].

Causes of Lateral Falls

Lateral falls [6] are defined as falling sideways relative to the frontal plane because of a lack of lateral stability, delayed postural control, and/or environmental factors [7]. Lateral stability can decrease because of age-related declines in physical and mental functions [8, 9] as well as the neurological factors hemiplegia [10] and progressive supranuclear palsy with motor paralysis [11]. Patients with these conditions or with progressive diseases require an assistive device for fall prevention and continuous rehabilitation. However, no orthotic or functional aid is currently available that can directly and immediately control dynamic balance on the frontal plane to prevent lateral falls. The occurrence frequency of lateral falls is increased by environmental factors that affect the lateral stability during walking, such as the slope of the walking surface [12]. Simulations using rigid-body models [13] showed that the occurrence of a fall is influenced by the relationship between the center of gravity (COG) of the body on the frontal plane and the base of support (BOS), the size of the BOS, the shape of the plantar surface, and the shape of the ground surface.

ASME Journal of Engineering and Science in Medical Diagnostics and Therapy. Received February 28, 2022;
Accepted manuscript posted July 22, 2022. doi:10.1115/1.4055040

Conventional Orthotic Therapies and Assistive Devices

Orthotic therapy and assistive devices are common interventions to compensate for the loss of function and to control involuntary movements during the gait cycle. Several types have been applied to assist with activities of daily living and rehabilitation. The ankle–foot orthosis immobilizes and supports the ankle joint in a functional position for walking. It is lightweight and wearable, but it also limits ankle movement and disturbs balance control in the frontal plane [14]. Exoskeleton-assist robotics for gait rehabilitation include HAL (CYBERDYNE Inc., Japan), Lokomat (Hocoma AG, Switzerland), and Ekso (Ekso Bionics, USA); these are actively controlled and provide power assistance when the muscular strength is insufficient during task-oriented and repetitive rehabilitation training. However, their excessive motor assistance or inhibition, weight and power demand as well as their highly specialized and complex operation and settings make them difficult for patients to operate, set up, and use independently. The above orthoses are usually used to control motion on the sagittal plane, such as assisting with propulsion or assisting joints with flexion and extension. However, no devices are currently available that assist or control the gait on the frontal plane or that compensate for lateral instability to prevent falls whereas many conventional orthoses are designed to improve anterior-posterior stability to fix the ankle to maintain dorsiflexion not to tripping.

Insole therapy is also available to improve lateral stability and uses the height and position of a lateral wedge placed outside the plantar surface, and it is recognized as a method for controlling gait [15, 16]. It is based on adjusting the direction of the

ASME Journal of Engineering and Science in Medical Diagnostics and Therapy. Received February 28, 2022;
Accepted manuscript posted July 22, 2022. doi:10.1115/1.4055040

ground reaction force (GRF), which causes a rotational force in the opposite direction of a lateral fall and simultaneously influences the alignment of the foot and lower leg muscles. This in turn promotes the activity of specific muscles [15]. Thus, it controls the gait by maximizing the effects of internal and external forces on the body simply by increasing the lateral height of the plantar surface [17]. However, this method is not applicable to conventional walking environments that require real-time adjustment. And also, it may cause difficulty to walk, or discomfort may be felt if the sole height is always raised up to a fixed height except when necessary.

Methods for Assessing Lateral Falls During the Gait Cycle

Several indices have been proposed for evaluating lateral falls in simulations of rigid-body models [13, 18], such as the relationships between the COG and center of pressure (COP) (i.e., COG–COP inclination angle and horizontal distance) [19-25], COG and BOS [26], and COG and BOS considering lateral acceleration [27]. In a clinical study, Murray et al. [28] showed that elderly participants with a history of falls had a significantly greater shift in the ML COG during the gait cycle than healthy young participants, which may also be an indicator of lateral stability. Ikai et al. [29] reported that patients with hemiplegia tended to fall on their affected side. Muscular activity is the main indicator of the internal postural control of the body against falls. Muscle contraction around the joint occurs in the direction opposing the falling moment to control instability caused by disturbances to the balance. Postural control against lateral instability depends on the ankle and hip strategies [30-33]. The ankle joint balance

ASME Journal of Engineering and Science in Medical Diagnostics and Therapy. Received February 28, 2022;
Accepted manuscript posted July 22, 2022. doi:10.1115/1.4055040

strategy on the frontal plane comprises inversion and eversion motions with the subtalar joint [34-36], which include the tibialis anterior (TA) and peroneus longus (PL) as protagonistic muscles in inversion and eversion, respectively [34, 37, 38]. For example, when a person falling to the side and leans outward due to the walking environment and posture, both the TA and PL increase their activity for postural control. In particular, maintaining posture against a falling moment on the frontal plane requires increasing the activity of the TA [34, 37, 38].

Objective

The Intelligent Foot Orthosis (IFO) was developed to control the plantar height in real-time to prevent lateral falls [17]. A preliminary evaluation [17] suggested that the IFO can prevent lateral falls when the lateral height of the plantar surface is always given. However, the effectiveness of the IFO at fall prevention when the plantar height is adjusted in real-time due to the walking motion has not been clarified. In addition, the effect of the IFO on muscular activity for postural control is not well understood. The objectives of this study were to verify experimentally the effectiveness of the IFO at fall prevention with real-time control of the lateral height of the plantar surface and to evaluate the immediate effects of wearing the IFO on the muscular activity associated with postural control to prevent lateral falls, particularly that of the TA.

MATERIALS AND METHODS

Description of the Intelligent Foot Orthosis

ASME Journal of Engineering and Science in Medical Diagnostics and Therapy. Received February 28, 2022;
Accepted manuscript posted July 22, 2022. doi:10.1115/1.4055040

The IFO was previously developed for real-time gait control through adjustment of the lateral height of the plantar surface [17]. The IFO and its design are shown in Fig. 1. A magnetorheological (MR) brake was developed to adjust the plantar height [17]. An MR fluid changes its yield shear stress when an external magnetic field is applied, and it is able to generate a relatively large amount of force from a small amount of power [39]. Figure 2 and Table 1 shows the components of the designed MR brake, including details on the piston and orifice. The MR brake has a double-rod-type damper structure [40], and the MR effect [41], which is dominated by friction forces, is used to hold the piston in position. The inner diameter of the orifice controls the flow of the MR fluid. When no current is applied, the piston moves up and down as the MR fluid flows through the orifice. Conversely, applying a current of 1.5 A generates a magnetic field around the orifice, which fixes the position of the piston at a plantar height of 5 mm. One AA battery (1.5V) provides sufficient power to control a load of approximately 10% of the body weight up to 125N on the area of the lateral sole during walking when current is applied [42]. A microcontroller (Arduino, Arduino Uno Rev3 A000066) is used as the controller, and an inertial measurement unit (Umemoto LLC, REES-01) is used as a sensor. In this study, the system was configured so that the current flowed when the road surface inclined more than 5° to the side during walking, which fixed the piston at the upper dead point.

The entire IFO system includes a shoe, which is worn on the affected side, weighs 745 g. It is within the weight range for use in clinical practice, as the commonly used mainstream brace for patients with hemiplegia and shoe weighs approximately 880 g

ASME Journal of Engineering and Science in Medical Diagnostics and Therapy. Received February 28, 2022;
Accepted manuscript posted July 22, 2022. doi:10.1115/1.4055040

[53]. A weight and placement of each part of the IFO that were determined so as not to affect the dorsiflexion of the ankle joint (Fig.1 (c)). To this end, a mobile battery for the controller (105 g) and AA batteries for the MR brake (70 g) were attached to the lower leg. As a result, COG rose by only 0.07% [54, 55] and have little influence on gait instability.

The IFO has a response time of approximately 0.20 s and is applicable to the gait cycle of 0.49 s [17]. Considering the literature [56-57], the IFO meets the requirement for patients with hemiplegia with the estimated gait cycle of 0.91 to 1.14 s and even fast-walking healthy adults with that of 0.51 s.

The static load capacity required for the MR brake is appropriately 4.5% of the whole weight of the human body in the configuration shown in Figure 1 considering the lever mechanism in the IFO, and 22.1 N for this subject [17, 42]. The MR brake with 125N at 1.5 A is capable of providing the required dynamic load capacity of 70 to 80 N acquired from a preliminary test for this subject.

Prevention of Lateral Falls During the Gait Cycle

Figure 3 shows the gait control mechanism of the IFO. When an electric current is applied, the MR brake is fixed to the upper dead point without piston displacement. When the current does not flow, the load on the weight-bearing device during the stance phase depresses the MR brake to its maximum piston displacement. It is then returned to the original height by the restoring force of the spring in the next swing phase.

ASME Journal of Engineering and Science in Medical Diagnostics and Therapy. Received February 28, 2022;
Accepted manuscript posted July 22, 2022. doi:10.1115/1.4055040

The height value is fixed at 5mm at the upper dead point when a current is applied, and the height is given by control when the slope lateral angle of the walkway becomes more than 5° (Fig.3). The height of 5 mm is determined based on the thickness (around 0.1 mm to 0.3 mm) of insoles in clinical use [58] and the maximum thickness (< 6 mm) that would not cause discomfort or foot disorders [59-60].

This system uses semi-active control rather than active control, as detailed in Figs. 4 and 5. The slope of the walking path is detected in real-time, and the lateral height of the plantar surface is controlled to adjust the direction of the GRF opposite of the falling moment during the stance phase. In other words, it controls the COG in the inward direction.

Experimental Conditions

The immediate effects of wearing the IFO on a laterally inclined walkway were compared based on COG and COP data to measure the gait and surface electromyography (EMG) data to measure the muscular activity. One healthy adult (38 years old, 158.5 cm, body weight 50.0 kg, BMI 19.9) with no history of orthopedic disorders in the observed lower extremities participated in this study. Gait data were collected from 10 trials under each of four walking conditions: (1) without IFO, (2) with IFO current-OFF, (3) with IFO current-ON, and (4) with IFO control-ON. Figures 3 and 4 detail the differences between these conditions. In addition, data without the IFO were acquired as supplementary data. In this study, the IFO was worn on one side and an

ASME Journal of Engineering and Science in Medical Diagnostics and Therapy. Received February 28, 2022;
Accepted manuscript posted July 22, 2022. doi:10.1115/1.4055040

experimental environment was established where the user would tend to fall to one side.

In the experiment, the right-side limb was observed. Under the "with IFO" conditions, the orthosis was placed on the right foot. To induce lateral instability, which is a stimulus for lateral falls, the walkway was 10° laterally inclined. Figure 6 shows the measurement environment.

Analysis

Mediolateral COG–COP Horizontal Distance

The Optotrak Certus® motion capture system (Northern Digital Inc., Canada), which has a resolution of 0.01 mm and accuracy of up to 0.1 mm, which is less than 0.5 mm when used from 5 m away, was used for gait analysis. As shown in Fig. 6, force plates (Advanced Mechanical Technology, Inc., USA) were used to measure the GRF. For three-dimensional gait analysis, infrared light-emitting diode markers were placed at 11 locations on the body based on anatomical landmarks: the bilateral greater trochanter, bilateral knee lateral joint space, bilateral lateral malleolus, bilateral tuberosity of the fifth metatarsal, bilateral acromion, and parietal. Nine infrared cameras at three locations were used for motion capture of these markers. The sampling frequency was 100 Hz, and the 3D position data of each marker were measured. The force plates were embedded in the floor, and the sampling frequency was 1000 Hz. The GRF meter was synchronized with the three-dimensional motion analysis system. Ten trials were conducted under each condition to acquire data. The COG and COP were calculated

ASME Journal of Engineering and Science in Medical Diagnostics and Therapy. Received February 28, 2022;
Accepted manuscript posted July 22, 2022. doi:10.1115/1.4055040

from the acquired 3D position data of each marker and the GRF data. ML COG–COP HD (Fig. 7) and the y_{COG}, $y_{COP_{flat}}$, $y_{COP_{slope}}$ on the lateral slope (Fig. 8) were calculated as follows [17]:

$$\text{ML COG} - \text{COP HD} = y_{COP_{slope}} - y_{COG} \tag{1}$$

Where the positive y-axis represents the right side of the direction of gait. $y_{COP_{slope}}$ is the y-coordinate of COP on the 10° lateral slope, and the COG coordinates, y_{COG}, are calculated from the positions of the 11 markers and the mass ratio of each body segment. y_{COG} is the y -coordinate of COG. $y_{COP_{slope}}$ is calculated by the following formula.

$$\left(y_0 - y_{COP_{slope}}\right)\tan 10° = \left(y_{COP_{flat}} - y_{COP_{slope}}\right) \cdot \frac{F_Z}{F_y} \tag{2}$$

$$y_{COP_{slope}} = \frac{y_0 \tan 10° - y_{COP_{flat}} \frac{F_Z}{F_y}}{\tan 10° - \frac{F_Z}{F_y}} \tag{3}$$

Here y_0 is the y-coordinate of the contact point between the slope and force plate, and F_y and F_z are the forces in y-axis and z-axis measured by the force plate respectively. $y_{COP_{flat}}$ is the y-coordinate of COP on the floor, which is calculated by the following formula.

ASME Journal of Engineering and Science in Medical Diagnostics and Therapy. Received February 28, 2022;
Accepted manuscript posted July 22, 2022. doi:10.1115/1.4055040

$$y_{COP_{flat}} = \frac{(M_x - F_y z_0)}{F_z} \quad (4)$$

M_x is the moment around the x-axis measured by the force plate and z_0 is the z-coordinate of its surface.

Surface Electromyography

Surface EMG (Biometrics Ltd, UK) was used to acquire the muscular activity of the TA and PL, which contribute to balance in the medial and lateral directions on the frontal plane. The soleus (Sol) was also measured to understand the relationship between the TA and PL. The muscles of the right lower limb were examined. The skin was rubbed and cleaned with an abrasive paste and alcoholic cotton to reduce skin impedance. Electrodes were then applied parallel to the direction of the muscle fibers in positions set according to Surface Electromyography for the Non-Invasive Assessment of Muscles (SENIAM) guidelines [43].

The amplified EMG signals were transferred to a PC via an analog/digital (A/D) converter. The electrodes (Biometrics Ltd, UK) (37 mm × 20 mm × 6 mm) were placed on the skin above the muscle being examined. The distance between electrodes was 20 mm. The stance phase was defined as the period when the vertical GRF was greater than 10 N. The middle of the stance phase was identified as the moment when the anterior and posterior GRF switched. A bandpass filter at 20–500 Hz was applied to the raw EMG data of the PL, TA, and Sol in the first half of the stance phase, and the root mean square (RMS) was calculated. The analysis was performed in Python, and general

ASME Journal of Engineering and Science in Medical Diagnostics and Therapy. Received February 28, 2022;
Accepted manuscript posted July 22, 2022. doi:10.1115/1.4055040

calculations were performed by using NumPy and math. NumPy and pandas were used for data management, and scipy.signal.butter and scipy.signal.filtfilt were used for signal processing.

Statistical Analysis

The mean and standard deviation were calculated for each condition and outcome measure, and one-way analysis of various and multiple comparisons were performed. The significance level was set to less than 0.05 ($p < 0.05$). The above procedures were statistically processed by using R.

RESULTS

Table 2 summarizes the results. There were no adverse events due to the use of the IFO, and no falls occurred in any trial.

Mediolateral COG–COP Horizontal Distance

As an example, Fig. 9 shows the ML COG–COP HD of one trial under the "without IFO" and "with IFO control-ON" conditions. As shown in Fig. 10, the mean values of the COG–COP HD were 66.65 ± 5.69 mm under the "without IFO" condition, 72.90 ± 5.91 mm under the "with IFO current-OFF" condition, 69.81 ± 5.97 mm under the "with IFO current-ON" condition, and 77.40 ± 4.56 mm under the "control-ON" condition. In the case of "with IFO control-ON", it was significantly higher ($p < 0.05$) compared to "without IFO" and "with IFO current-ON".

ASME Journal of Engineering and Science in Medical Diagnostics and Therapy. Received February 28, 2022;
Accepted manuscript posted July 22, 2022. doi:10.1115/1.4055040

Mean and Peak RMS in EMG

Figure 11 shows examples of the TA and PL EMG data from a gait trial. As shown in Fig. 12, in the type of lateral inclined walkway, the mean RMS of the TA in the "with IFO current-ON" (0.035 ± 0.009 V) and "control-ON" (0.036 ± 0.010 V) conditions in the first half of the stance phase were significantly lower ($p < 0.01$) than in the "without IFO" (0.065 ± 0.018V) condition. For PL, in "with IFO current-OFF" (0.027± 0.007V), it was significantly lower ($p < 0.05$) than in "without IFO" (0.098 ± 0.018). There was an also significant difference in peak RMS between the "without IFO" and "with IFO current-OFF" conditions for the PL. However, no significant difference was found for the TA and Sol in peak RMS.

DISCUSSION

In this study, experiments were performed to evaluate the effectiveness of the IFO at lateral fall prevention. The IFO had immediate effects on kinematic parameters such as the COG and COP and on physical functions such as muscular activity. We focus on TA as for protagonist of ankle inversion which works for preventing lateral fall. No adverse events occurred during, before, or after the experiments. The effectiveness of the IFO at lateral fall prevention was demonstrated by the following results.

Effects of IFO on Preventing Lateral Falls

As shown in Fig. 10, the COG–COP HD was significantly greater under the "with IFO control-ON" condition than the "without IFO" condition and was significantly

ASME Journal of Engineering and Science in Medical Diagnostics and Therapy. Received February 28, 2022;
Accepted manuscript posted July 22, 2022. doi:10.1115/1.4055040

greater under the "control-ON" condition than the "current-ON" condition. A smaller COG–COP HD means greater lateral displacement of the COG relative to the COP, which indicates instability [23]. Therefore, patients with reduced lateral stability such as the elderly maintain a larger value than healthy individuals because they adjust their posture to a stable position to prevent falls [23, 24]. Increasing the ML COG–COP HD greater the angle between the COG–COP HD and floor, which suggests that wearing the IFO reduces the chance of a lateral fall.

The results showed that the "control-ON" condition had a significantly greater effect than the "current-ON" condition, which suggests that the former is more effective at fall prevention. In the first half of the stance phase, the piston was fixed at the upper dead point in both cases, and the results here showed that the "control-ON" was more significant than the "current-ON" condition. The main difference between the "with IFO current-ON" and "with IFO control-ON" conditions was that the plantar height was always given throughout the walking trial on either level ground or the laterally inclined walkway for the former. The mechanism remains unclear at this stage, but the presence or absence of plantar height control from before the control interval may carry over and effect physical functions. The subjects commented that they felt sensory discomfort in the sole because of the outer part of the plantar being continuously raised even when walking on flat ground under the "current-ON" condition. Previous studies have reported that sensory stimulation and change of the plantar surface by a few millimeters due to a protrusion or partial insole can change the gait and posture, although this can lead to improved stability depending on the usage [44-47]. The

ASME Journal of Engineering and Science in Medical Diagnostics and Therapy. Received February 28, 2022;
Accepted manuscript posted July 22, 2022. doi:10.1115/1.4055040

sensations have also been reported to differ among individuals [17, 45]. Thus, in addition to real-time control, the system should adapt to the wearer's posture and sensations when walking on level ground. Further case studies are needed on how wearers adapt to using the IFO.

Effectiveness of IFO in muscle activity

As shown in Fig. 12, the EMG results indicated that TA activity under the "with IFO current-ON" and "control-ON" conditions were significantly reduced than the "without IFO" condition. This suggests that the IFO may assist with postural control together with the TA. For a normal gait cycle without any assistance or aid, both the TA and PL showed increased activity on the lateral inclined walkway compared to on a level surface [48]. Based on the estimated muscular activity from the directions of the GRF and joint moment [49], the ankle joint is mainly responsible for lateral balance control [32]. For an inclined walkway, the TA activity should increase to maintain the posture in the opposite direction and avoid falling on the frontal plane [48]. Previous studies have shown significantly increased TA activity and decreased PL activity after lateral fall stimulation during a gait cycle in a restricted environment [50, 51]. This suggests that any external force or stimulus that reduces lateral stability is likely to increase TA activity significantly under the "without IFO" condition. The ML COG–COP HD results showed that the posture was tilted in a direction that prevented falling under the "with IFO current-ON" and "with IFO control-ON" conditions, which suggests that wearing the IFO may reduce the likelihood of falling. It would unclear whether this might due to

ASME Journal of Engineering and Science in Medical Diagnostics and Therapy. Received February 28, 2022;
Accepted manuscript posted July 22, 2022. doi:10.1115/1.4055040

posture control by TA contraction or the effect of the IFO. However, the TA activity during the gait cycle predominantly decreased under the "with IFO current-ON" and "with IFO control-ON" conditions, which suggests that the IFO helped prevent falling and reduced the demand for muscle activity required for postural control. Thus, the IFO was demonstrated to help prevent lateral falls.

These results are clinically relevant because relieving the muscular activity for ankle inversion can be beneficial for particular neurological conditions [52]. For stroke patients, continuous and excessive muscle contraction may worsen spasticity, which is related to control of voluntary movements [50]. In such cases, using the IFO to support the TA may result in better gait control. Thus, preventing lateral falls while controlling the TA muscular activity may be clinically beneficial. The activity of this muscles can be used as an indicator of the patient's functional status for clinicians to consider when prescribing the IFO.

Limitations

The limitations of this study are as follows:

- The mechanism behind the different effects of the "with IFO current-ON" and "with IFO control-ON" conditions is unexplained and needs further investigation.
- For the surface EMG, only the three main superficial muscles of the lower limb were measured. Other muscles are involved in lateral stability, and further assessment is needed to examine the internal forces.

ASME Journal of Engineering and Science in Medical Diagnostics and Therapy. Received February 28, 2022;
Accepted manuscript posted July 22, 2022. doi:10.1115/1.4055040

- This study was carried out in an indoor laboratory. Further research needs to be conducted in outdoor environments and community settings to evaluate the effectiveness of the IFO at lateral fall prevention under actual application conditions.
- The present study was only a preliminary experimental verification of a proof of concept. Because of the small number of cases considered, further case studies, including clinical use, need to be conducted.
- The relationship between the stroke of IFO and ML COG-COP HD is not yet clear. If the stroke length is too short, the effect on posture is small; if it is too large, it causes the foot to fall in the opposite direction. It indicates that controlling the height with regard to the range is significant and this should be considered for further study.

CONCLUSIONS

This study experimentally assessed the effectiveness of the developed IFO for lateral fall prevention. The following findings were obtained:

1. The IFO's potential to effectively prevent lateral falls under control is indicated by the result of ML COP-COG HD which significantly increases in the "with IFO control-ON" condition compared to the "without IFO" and "with IFO current-ON" conditions.

2. The "with IFO current-ON" and "with IFO control-ON" conditions significantly reduced TA activity compared to the "without IFO" condition, which suggests that wearing the IFO may assist with TA muscular activity during postural control.

ASME Journal of Engineering and Science in Medical Diagnostics and Therapy. Received February 28, 2022;
Accepted manuscript posted July 22, 2022. doi:10.1115/1.4055040

ACKNOWLEDGMENT

The authors especially thank Mr. Kohei Morimura, a member of the research team who developed the IFO; Mr. Hiroki Tanabe and Ms. Yuri Kuroki for technical assistance with the experiments; and Mr. James Duckworth for contributing language support.

FUNDING

This study was supported partly by the "YNU Diversity Research Grant" under MEXT Funds for the Development of Human Resources in Science and Technology, Japan – "Initiative for Realizing Diversity in the Research Environment (Collaboration Type)" and the Joint Research Promotion Program of Graduate School of Environment and Information Sciences, Yokohama National University, Japan, Joint Research Project "Type C."

ASME Journal of Engineering and Science in Medical Diagnostics and Therapy. Received February 28, 2022;
Accepted manuscript posted July 22, 2022. doi:10.1115/1.4055040

NOMENCLATURE

IFO	Intelligent Foot Orthosis
TA	tibia anterior
PL	peroneus longus
ML COG–COP HD	mediolateral center of gravity and center of pressure horizontal distance
EMG	electromyography
COG	center of gravity
COP	center of pressure
BOS	base of support
GRF	ground reaction force

ASME Journal of Engineering and Science in Medical Diagnostics and Therapy. Received February 28, 2022;
Accepted manuscript posted July 22, 2022. doi:10.1115/1.4055040

REFERENCES

[1] Suzuki, T., 2002, "Spasticity Control in Exercise Therapy," Journal of Clinical Rehabilitation, 11, pp. 907-912. https://search.jamas.or.jp/link/ui/2003080104

[2] Bergen, G., Stevens, M. R., and Burns, E. R., 2016, "Falls and Fall Injuries Among Adults Aged ≥65 Years - United States, 2014," MMWR Morb. Mortal Wkly. Rep., **65**(37), pp. 993-998. DOI:10.15585/mmwr.mm6537a2

[3] Forster, A., and Young, J., 1995, "Incidence and Consequences of Falls Due to Stroke: A Systematic Inquiry," BMJ, **311**(6997), pp. 83-86. DOI:10.1136/bmj.311.6997.83

[4] Parkkari, J., Kannus, P., Palvanen, M., Natri, A., Vainio, J., Aho, H., Vuori, I., and Järvinen, M., 1999, "Majority of Hip Fractures occur as a Result of a Fall and Impact on the Greater Trochanter of the Femur: A Prospective Controlled Hip Fracture Study with 206 Consecutive Patients," Calcif.Tissue Int., **65**(3), pp. 183-187. DOI:10.1007/s002239900679

[5] Hayes, W. C., Myers, E. R., Morris, J. N., Gerhart, T. N., Yett, H. S., and Lipsitz, L. A., 1993, "Impact Near the Hip Dominates Fracture Risk in Elderly Nursing Home Residents who Fall," Calcif. Tissue Int., **52**(3), pp. 192-198. DOI:10.1007/bf00298717

[6] Moon, Y., and Sosnoff, J. J., 2017, "Safe Landing Strategies During a Fall: Systematic Review and Meta-Analysis," Arch. Phys. Med. Rehabil., **98**(4), pp. 783-794. DOI:10.1016/j.apmr.2016.08.460

[7] Dionyssiotis, Y., 2012, "Analyzing the Problem of Falls among Older People," International Journal of General Medicine, **5**, p. 805. DOI:10.2147/ijgm.s32651

[8] Pyykkö, I., Jäntti, P., and Aalto, H., 1990, "Postural Control in Elderly Subjects," Age Ageing, **19**(3), pp. 215-221. DOI:10.1093/ageing/19.3.215

[9] Schrager, M. A., Kelly, V. E., Price, R., Ferrucci, L., and Shumway-Cook, A., 2008, "The Effects of Age on Medio-lateral Stability during Normal and Narrow Base Walking," Gait Posture, **28**(3), pp. 466-471. DOI:10.1016/j.gaitpost.2008.02.009

[10] van Dijk, M. M., Sandstad, S., Ghosh, N., Dejaeger, E., Beyens, H., and Verheyden, G., 2015, "Diagonal and Lateral Limits of Stability Post Stroke show a Significant Relation with Gait, Balance and the Risk of Falling," Physiotherapy, **101**, pp. e1572-e1573. DOI:10.1016/j.physio.2015.03.1575

[11] Amano, S., Skinner, J. W., Lee, H. K., Stegemöller, E. L., Hack, N., Akbar, U., Vaillancourt, D., McFarland, N. R., and Hass, C. J., 2015, "Discriminating Features of Gait Performance in Progressive Supranuclear Palsy," Parkinsonism Relat. Disord., **21**(8), pp. 888-893.

[12] Ahn, J., Sakurai, S., and Kim, H., 2007, "Comparison of Muscular Activity of the Lower Limb While Running on Inclined Surfaces," Japanese Journal of Physical Fitness and Sports Medicine, **56**(1), pp. 167-178. DOI:10.7600/jspfsm.56.167

[13] Morimura, K., Yamamoto, R., and Shiraishi, T., 2020, "A Study of a Fall Prevention System for Patients with Walking Disabilities," The Proceedings of the Dynamics & Design Conference, p. 423. DOI:10.1299/jsmedmc.2020.423

[14] Delafontaine, A., Gagey, O., Colnaghi, S., Do, M. C., and Honeine, J. L., 2017, "Rigid Ankle Foot Orthosis Deteriorates Mediolateral Balance Control and Vertical Braking during Gait Initiation," Front. Hum. Neurosci., **11**, p. 214. DOI:10.3389/fnhum.2017.00214

[15] Ohata Koji, I. N., and Takemura T., 2004, "The Effect of Lateral Wedged Insoles for Gait on Electromyographic Analysis," The Journal of Japanese Physical Therapy Association, **31**(3), pp. 175-181. DOI:10.15063/rigaku.KJ00001021068

[16] Khamis, S., and Yizhar, Z., 2007, "Effect of Feet Hyperpronation on Pelvic Alignment in a Standing Position," Gait Posture, **25**(1), pp. 127-134. DOI:10.1016/j.gaitpost.2006.02.005

[17] Kohei, M., Rieko, Y., and Toshihiko, S., 2021, "Orthosis with a Controllable Plantar Height for Fall Prevention using a Compact Magnetorheological Fluid Brake," Journal of intelligent material systems and structures, **33**(7), pp. 928-941. DOI:10.1177/1045389X211038710

[18] Morimura, K., Yamamoto, R., and Shiraishi, T., 2020, "Control of Plantar Height by an MR Fluid Brake for Fall Prevention of Patients with Walking Disabilities," The Proceedings of the International Conference on Motion and Vibration Control, **2020**(15), p. 10067. DOI:10.1299/jsmeintmovic.2020.15.10067

[19] Choi, A., Jung, H., and Mun, J. H., 2019, "Single Inertial Sensor-Based Neural Networks to Estimate COM-COP Inclination Angle During Walking," Sensors, **19**(13). DOI:10.3390/s19132974

[20] Rogers, M. W., Hedman, L. D., Johnson, M. E., Cain, T. D., and Hanke, T. A., 2001, "Lateral Stability during Forward-induced Stepping for Dynamic Balance Recovery in Young and Older Adults," J. Gerontol. A Biol. Sci. Med. Sci., **56**(9), pp. M589-594. DOI:10.1093/gerona/56.9.m589

[21] Mousavi, S. H., van Kouwenhove, L., Rajabi, R., Zwerver, J., and Hijmans, J. M., 2021, "The Effect of Changing Mediolateral Center of Pressure on Rearfoot Eversion during Treadmill Running," Gait Posture, **83**, pp. 201-209. DOI:10.1016/j.gaitpost.2020.10.032

[22] Lee, Y. J., Liang, J. N., Chen, B., and Aruin, A. S., 2019, "Characteristics of Medial-Lateral Postural Control while Exposed to the External Perturbation in Step Initiation," Sci. Rep., **9**(1), p. 16817. DOI:10.1038/s41598-019-53379-9

[23] Lee, H. J., and Chou, L. S., 2006, "Detection of Gait Instability using the Center of Mass and Center of Pressure Inclination Angles," Arch. Phys. Med. Rehabil., **87**(4), pp. 569-575. DOI:10.1016/j.apmr.2005.11.033

[24] Chen, C.-J., and Chou, L.-S., 2007, "Center of Mass and Ankle Inclination Angles: An Alternative Detection of Gait Instability," Journal of Biomechanics, **40**, p. S286. DOI: 10.1016/S0021-9290(07)70282-8

[25] Lee, P.-A., Wu, K.-H., Lu, H.-Y., Su, K.-W., Wang, T.-M., Liu, H.-C., and Lu, T.-W., 2021, "Compromised Balance Control in Older People with Bilateral Medial Knee Osteoarthritis During Level Walking," Sci. Rep., **11**(1), p. 3742. DOI:10.1038/s41598-021-83233-w

[26] Fujimoto, M., Bair, W. N., and Rogers, M. W., 2015, "Center of Pressure Control for Balance Maintenance During Lateral Waist-pull Perturbations in Older Adults," J. Biomech., **48**(6), pp. 963-968. DOI:10.1016/j.jbiomech.2015.02.012

[27] Itami, S., 2022, "A Study of an Orthosis with Controllable Plantar Height by a Compact MR Brake for Fall Prevention of People with Walking Disabilities," Thesis, Yokohama National University, Kanagawa, JP.

[28] Murray, M. P., Kory, R. C., and Clarkson, B. H., 1969, "Walking Patterns in Healthy Old Men," J. Gerontol., **24**(2), pp. 169-178. DOI:10.1093/geronj/24.2.169

[29] Ikai, T., Kamikubo, T., Takehara, I., Nishi, M., and Miyano, S., 2003, "Dynamic Postural Control in Patients with Hemiparesis," Am. J. Phys. Med. Rehabil., **82**(6), pp. 463-469; quiz 470-462, 484. PMID: 12820790

[30] Matjačić, Z., Zadravec, M., and Olenšek, A., 2020, "Biomechanics of In-Stance Balancing Responses Following Outward-Directed Perturbation to the Pelvis During Very Slow Treadmill Walking Show Complex and Well-Orchestrated Reaction of Central Nervous System," Frontiers in Bioengineering and Biotechnology, **8**. DOI:10.3389/fbioe.2020.00884

[31] Blenkinsop, G. M., Pain, M. T. G., and Hiley, M. J., 2017, "Balance Control Strategies During Perturbed and Unperturbed Balance in Standing and Handstand," R. Soc. Open Sci., **4**(7), p. 161018. DOI:10.1098/rsos.161018

[32] Hashimoto, M., and Nakae, N., 2001, "Motor Skill and Physical Therapy. Motor Control of Body from the Viewpoint of Foot," Rigakuryoho Kagaku, **16**(3), pp. 123-128. DOI:10.1589/rika.16.123

ASME Journal of Engineering and Science in Medical Diagnostics and Therapy. Received February 28, 2022;
Accepted manuscript posted July 22, 2022. doi:10.1115/1.4055040

[33] Yagi, M., Suzuki, K., Anan, M., and Shinkoda, K., 2012, "Influences of Functional Ankle Instability on Postural Control during Transitioning to One-leg Standing," Rigakuryoho Kagaku, **27**(4), pp. 373-377. DOI:10.1589/rika.27.373

[34] Pheasant, S. T., 1981, "A Review of: "Human Walking". V. T. Inman, H.J. Ralston, and F. Todd, eds., (Baltimore, London: Williams & Wilkins, 1981.) [pp. 154.]," Ergonomics, **24**(12), pp. 969-976. DOI:10.1080/00140138108924919

[35] Brockett, C. L., and Chapman, G. J., 2016, "Biomechanics of the Ankle," Orthopaedics and Trauma, **30**(3), pp. 232-238. DOI:10.1016/j.mporth.2016.04.015

[36] Michael, J. M., Golshani, A., Gargac, S., and Goswami, T., 2008, "Biomechanics of the Ankle Joint and Clinical Outcomes of Total Ankle Replacement," Journal of the Mechanical Behavior of Biomedical Materials, **1**(4), pp. 276-294. DOI:10.1016/j.jmbbm.2008.01.005

[37] Mansfield, P. J., and Neumann, D. A., 2019, "Chapter 11 - Structure and Function of the Ankle and Foot," Essentials of Kinesiology for the Physical Therapist Assistant (Third Edition), P. J. Mansfield and D. A. Neumann, eds., Mosby, St. Louis (MO), pp. 311-350. ISBN: 978-0323544986

[38] Neumann, D. A., 2010, *Kinesiology of the Musculoskeletal System: Foundations for Rehabilitation*, Elsevier, Missouri, US. ISBN: 978-0323287531

[39] Shiraishi, T., and Morishita, S., 2004, "Measurements of Typical Characteristics of MR Fluids and Their Application to Design of MR Devices Considering Working Modes," Transactions of the Japan Society of Mechanical Engineers Series C, **70**(696), pp. 2308-2314. DOI:10.1299/kikaic.70.2308

[40] Shiraishi, T., Sakuma, T., and Morishita, S., "Design and Performance Verification of Variable Dampers Using MR Fluid." International Mechanical Engineering Congress and Exposition, **37130**, 989-994. DOI: 10.1115/IMECE2003-41346

[41] Sarkar, C., and Hirani, H., 2015, "Effect of Particle Size on Shear Stress of Magnetorheological Fluids," Smart Science, **3**(2), pp. 65-73. DOI:10.1080/23080477.2015.11665638

[42] Yamamoto, R., Morimura, K., and Shiraishi T., "A Feasibility Study of an Intelligent Fall Prevention System: A Sideways Fall Dynamic Model and the Effect of Lateral Insole " Proc. World Physiotherapy Congress 2021, PO-00361.

[43] "The SENIAM project (Surface Electromyography for the Non-Invasive Assessment of Muscles),"Sensor Placement". http://www.seniam.org/

[44] Kenny, R. P. W., Eaves, D. L., Martin, D., Hatton, A. L., and Dixon, J., 2019, "The Effects of Textured Insoles on Quiet Standing Balance in Four Stance Types With and

ASME Journal of Engineering and Science in Medical Diagnostics and Therapy. Received February 28, 2022;
Accepted manuscript posted July 22, 2022. doi:10.1115/1.4055040

Without Vision," BMC Sports Science, Medicine and Rehabilitation, **11**(1), p. 5. DOI:10.1186/s13102-019-0117-9

[45] Perry, S. D., Radtke, A., McIlroy, W. E., Fernie, G. R., and Maki, B. E., 2008, "Efficacy and Effectiveness of a Balance-enhancing Insole," J Gerontol A Biol Sci Med Sci, **63**(6), pp. 595-602. DOI:10.1093/gerona/63.6.595

[46] Eils, E., Streyl, M., Linnenbecker, S., Thorwesten, L., Völker, K., and Rosenbaum, D., 2004, "Characteristic Plantar Pressure Distribution Patterns during Soccer-specific Movements," Am J Sports Med, **32**(1), pp. 140-145. DOI:10.1177/0363546503258932

[47] Okoba, R., Hasegawa, M., Yoshizuka, H., Honda, Y., Egoshi, S., Mitsutake, T., and Asami, T., 2018, "Effects of a Perceptual Stimulus Insole on Foot Dynamics during Gait," Rigakuryoho Kagaku, **33**(2), pp. 343-346. DOI:10.1589/rika.33.343

[48] Bavdek, R., Zdolšek, A., Strojnik, V., and Dolenec, A., 2018, "Peroneal Muscle Activity during Different Types of Walking," J Foot Ankle Res, **11**, p. 50. DOI:10.1186/s13047-018-0291-0

[49] Fujisawa, H., 2009, Observational Motion Analysis Practice Note, Ishiyaku Publishers Inc. ISBN:978-4-263-21325-4

[50] Suzuki, T., 2002, "Spasticity Control in Exercise Therapy," Journal of Clinical Rehabilitation, **11**, pp. 907-912. https://search.jamas.or.jp/link/ui/2003080104

[51] Fettrow, T., DiBianca, S., Vanderlinde dos Santos, F., Reimann, H., and Jeka, J., 2020, "Flexible Recruitment of Balance Mechanisms to Environmental Constraints During Walking," Frontiers in Virtual Reality, **1**. DOI:10.3389/frvir.2020.00005

[52] Goto, J., 2003, "The Control of Muscle Tone," Journal of Kansai Physical Therapy, **3**, pp. 21-31. DOI:10.11354/jkpt.3.21

[53] Gait Solution, Pacific Supply Co., Ltd, accessed Feb 19, 2022, https://www.p-supply.co.jp/data/files/00001157-1.pdf

[54] Winter, D. A., 2009, Biomechanics and motor control of human movement, Wiley., pp. 83-91. ISBN:978-0470398180

[55] Nakamura R, Saito H, and H, N., 2007, Fundamental kinesiology, Ishiyaku Publishers Inc., pp. 348-358.ISBN: 978-4263211533

[56] Kondoh, S., Araki, S., and Kaji, K., 1995, "Relationship among Walking Speed, Stride Length, and Cadence in Hemiplegic Patients," Rigakuryoho kagaku, 10(1), pp. 11-14. DOI:10.1589/rika.10.11:10.1589/rika.10.11

ASME Journal of Engineering and Science in Medical Diagnostics and Therapy. Received February 28, 2022;
Accepted manuscript posted July 22, 2022. doi:10.1115/1.4055040

[57] Sekiya, N., 1996, "The invariant relationship between step length and step rate during free walking," J Hum Move Studies, 30, pp. 241-257. https://cir.nii.ac.jp/crid/1570572700080767744

[58] Iritani M., 2011, Iritani shiki sokuteiban kisohen, Publisher of Motion and Medical. ISBN: 978-4904862025

[59] Collins, N., Crossley, K., Beller, E., Darnell, R., McPoil, T., and Vicenzino, B., 2008, "Foot orthoses and physiotherapy in the treatment of patellofemoral pain syndrome: randomised clinical trial," BMJ, 337. DOI:p.a1735.10.1136/bmj.a1735:10.1136/bmj.a1735

[60] Eng, J. J., and Pierrynowski, M. R., 1993, "Evaluation of soft foot orthotics in the treatment of patellofemoral pain syndrome," Phys Ther, 73(2), pp. 62-68. DOI:discussion 68-70. 10.1093/ptj/73.2.62:10.1093/ptj/73.2.62

ASME Journal of Engineering and Science in Medical Diagnostics and Therapy. Received February 28, 2022;
Accepted manuscript posted July 22, 2022. doi:10.1115/1.4055040

FIGURE CAPTIONS LIST

Fig. 1	Intelligent Foot Orthosis (IFO) [17] (a) Name of each component and its mass. (b) Structure of the load bearing device. (c) Position of each component on the lower limb.
Fig. 2	Schematic diagram of the MR brake [17]
Fig. 3	Gait control mechanism of the IFO. The timing of height adjustment during the gait cycle is shown. IC: initial contact, LR: loading response, MSt: mid-stance, TSt: terminal Stance, ISw: initial swing, MSw: mid-swing, TSw: terminal swing.
Fig. 4	Plantar height control mechanism in the stance phase (a) shows the current-OFF and control-ON states (non-targeted phase) of the IFO. The piston drops to the lower dead point as soon as the orthotic side of the foot starts to load in the IC, and the plantar height is not controlled. (b) shows the current-ON and control-ON states (controlled phase) from the IC to MSt. The piston is fixed at the height of the upper dead point (7.0 mm raised height on the lateral side of the plantar midfoot) during the step from LR to MSt. By increasing the height of the plantar surface of the midfoot by 5.0 mm, the direction of the GRF is changed to oppose the fall moment.
Fig. 5	Piston displacement in the swing phase. After dropping to the lower dead point in the previous stance phase, the piston is returned to the upper

ASME Journal of Engineering and Science in Medical Diagnostics and Therapy. Received February 28, 2022;
Accepted manuscript posted July 22, 2022. doi:10.1115/1.4055040

	dead point in the subsequent stance phase by the spring's restoring force. Alternatively, the piston is always fixed at the upper dead point in the current-ON state.
Fig. 6	Experimental setup. (Left) Overview of the experimental environment. The Optotrak Certus Motion Capture System (Northern Digital Inc.) and force plates (AMTI Inc.) were used for 3D gait analysis, and surface electromyography (EMG) (Biometrics Ltd.) was used for EMG analysis. A lateral inclined platform on a stationary force plate was used as a lateral walkway. (Right) Walking test being performed. All data of force plate were acquired from the first force plate on the right-hand side with respect to the direction of walking.
Fig. 7	ML COG–COP HD in the stance phase. ML COG-COP HD decreases when posture tilts laterally (posterior view).
Fig. 8	COG and COP on a lateral slope
Fig. 9	Example results for the ML COG–COP HD
Fig. 10	ML COG–COP HD
Fig. 11	Example results of a gait trail with TA and PL EMG data under the "without IFO" and "with IFO control-ON" conditions. The blue line shows the timing for dividing the stance phase. BP: bandpass filter, RMS: root mean square.
Fig. 12	Mean RMS of the EMG for the tibia anterior (TA)

ASME Journal of Engineering and Science in Medical Diagnostics and Therapy. Received February 28, 2022;
Accepted manuscript posted July 22, 2022. doi:10.1115/1.4055040

Fig. 1

(a)

Mass of IFO	Value
Shoe	250g
MR brake	128g
Spring	17g
Controller and inertial measurement unit	70g
Loading device	105g
Battery(AA batteries)	70g
Mobile battery	105g
Total	745g

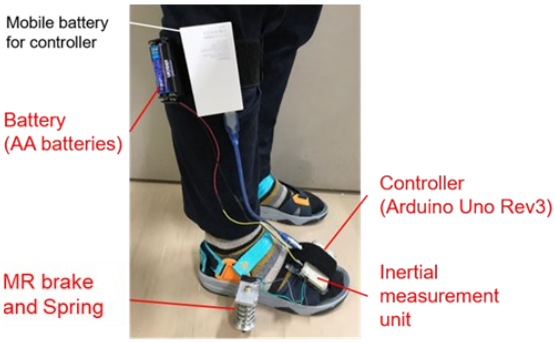

(b)

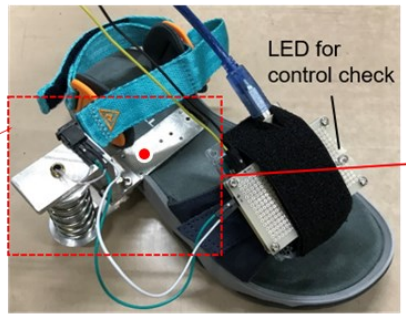

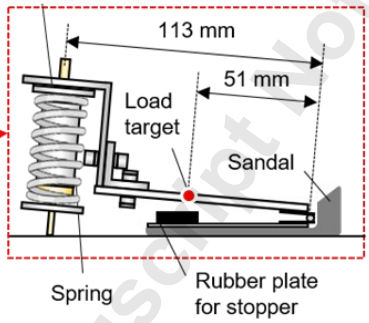

(C)

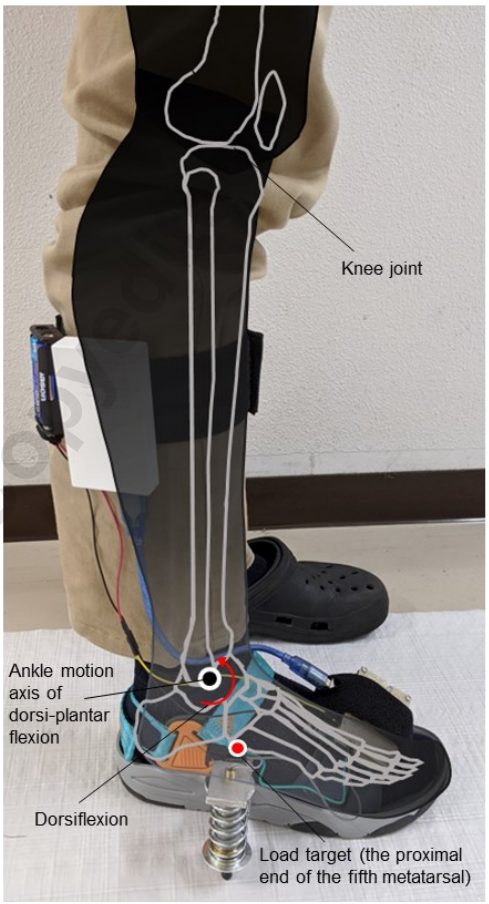

ASME Journal of Engineering and Science in Medical Diagnostics and Therapy. Received February 28, 2022;
Accepted manuscript posted July 22, 2022. doi:10.1115/1.4055040

Fig. 2

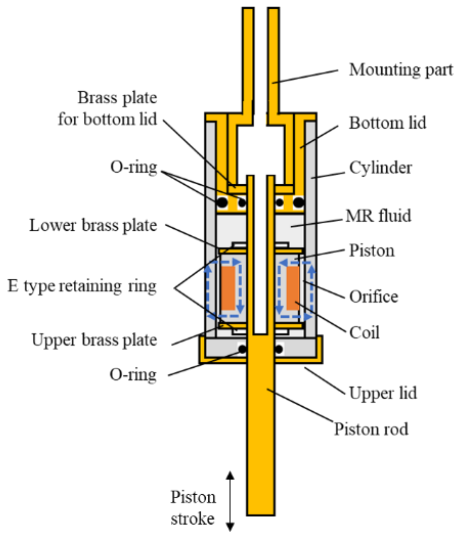

ASME Journal of Engineering and Science in Medical Diagnostics and Therapy. Received February 28, 2022;
Accepted manuscript posted July 22, 2022. doi:10.1115/1.4055040

Fig. 3

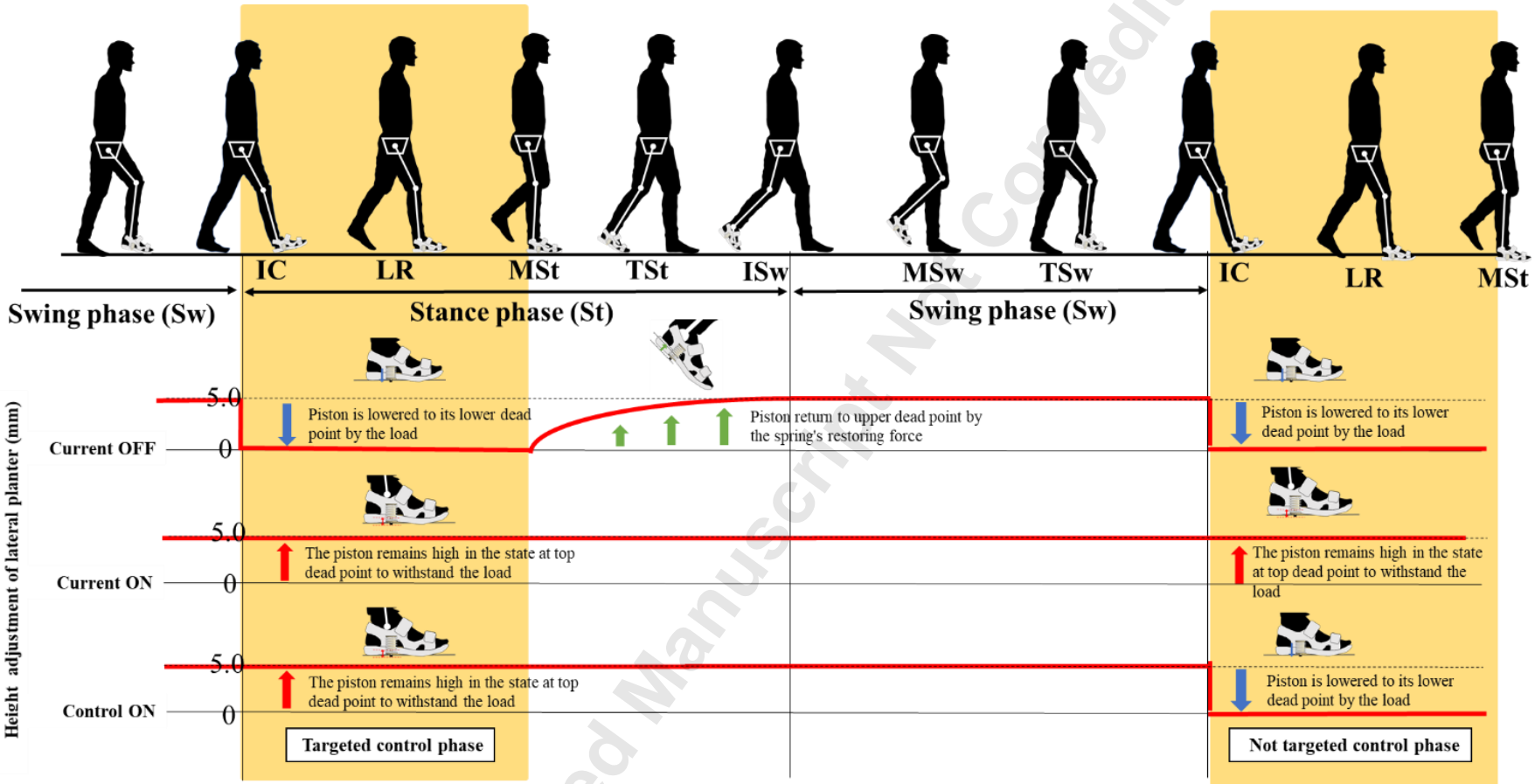

ASME Journal of Engineering and Science in Medical Diagnostics and Therapy. Received February 28, 2022;
Accepted manuscript posted July 22, 2022. doi:10.1115/1.4055040

Fig. 4

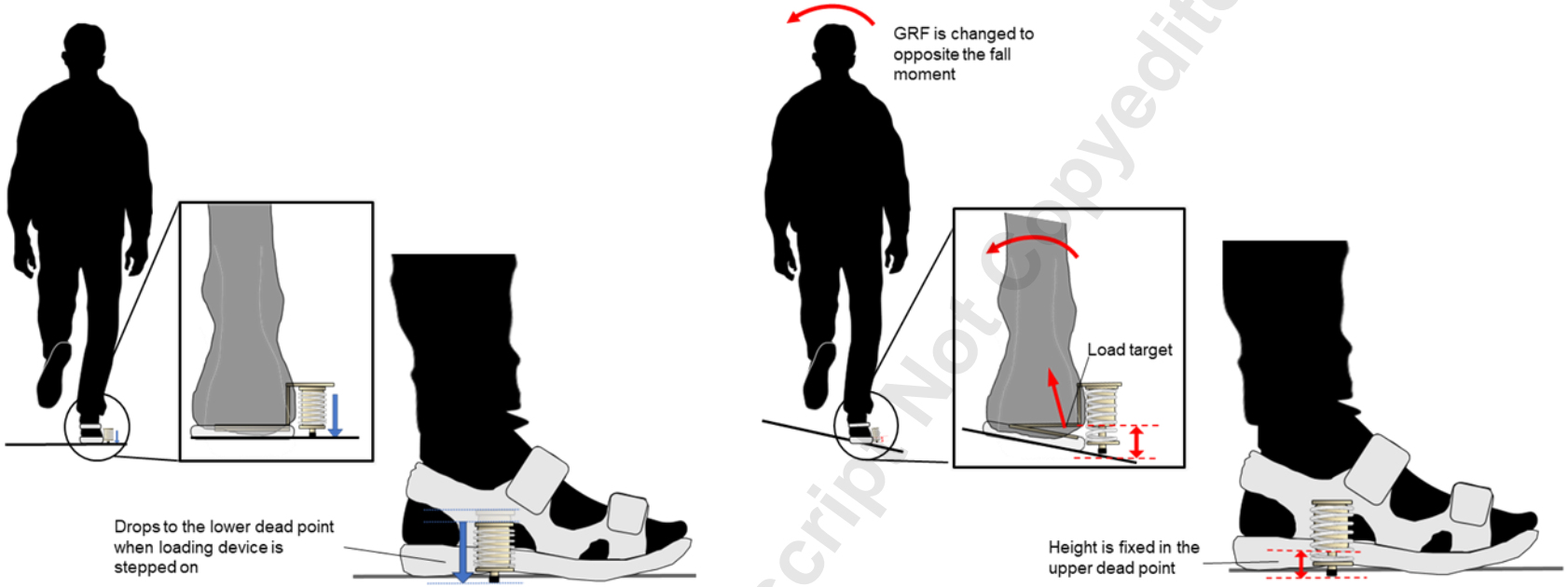

(a) Current-OFF and Current/Control-ON (Not-targeted phase)

(b) Current-ON and Current/Control-ON (targeted phase)

ASME Journal of Engineering and Science in Medical Diagnostics and Therapy. Received February 28, 2022;
Accepted manuscript posted July 22, 2022. doi:10.1115/1.4055040

Fig. 5

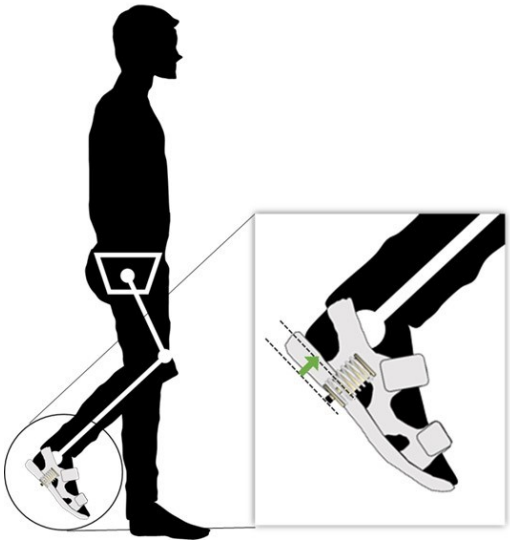

ASME Journal of Engineering and Science in Medical Diagnostics and Therapy. Received February 28, 2022;
Accepted manuscript posted July 22, 2022. doi:10.1115/1.4055040

Fig. 6

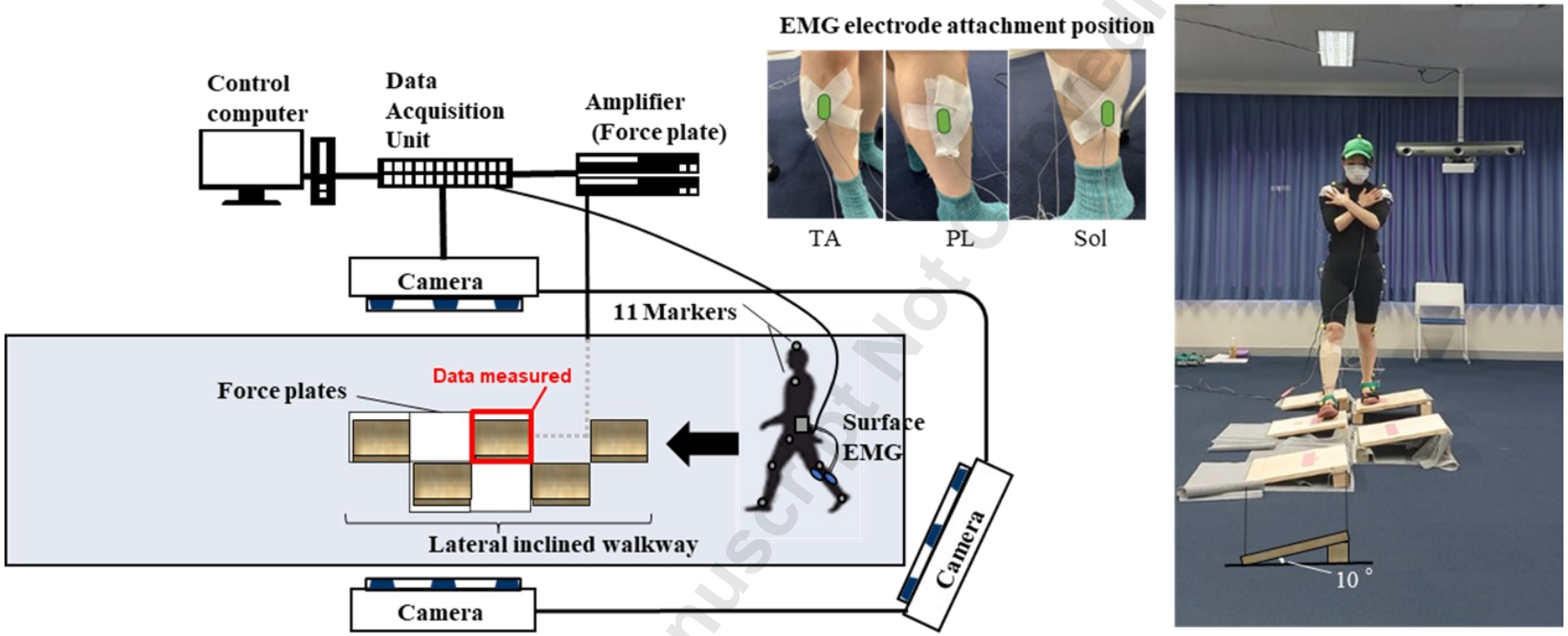

ASME Journal of Engineering and Science in Medical Diagnostics and Therapy. Received February 28, 2022;
Accepted manuscript posted July 22, 2022. doi:10.1115/1.4055040

Fig. 7

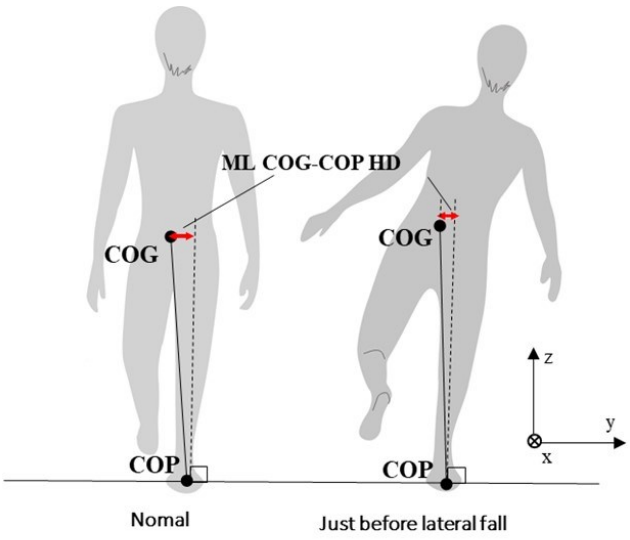

ASME Journal of Engineering and Science in Medical Diagnostics and Therapy. Received February 28, 2022;
Accepted manuscript posted July 22, 2022. doi:10.1115/1.4055040

Fig. 8

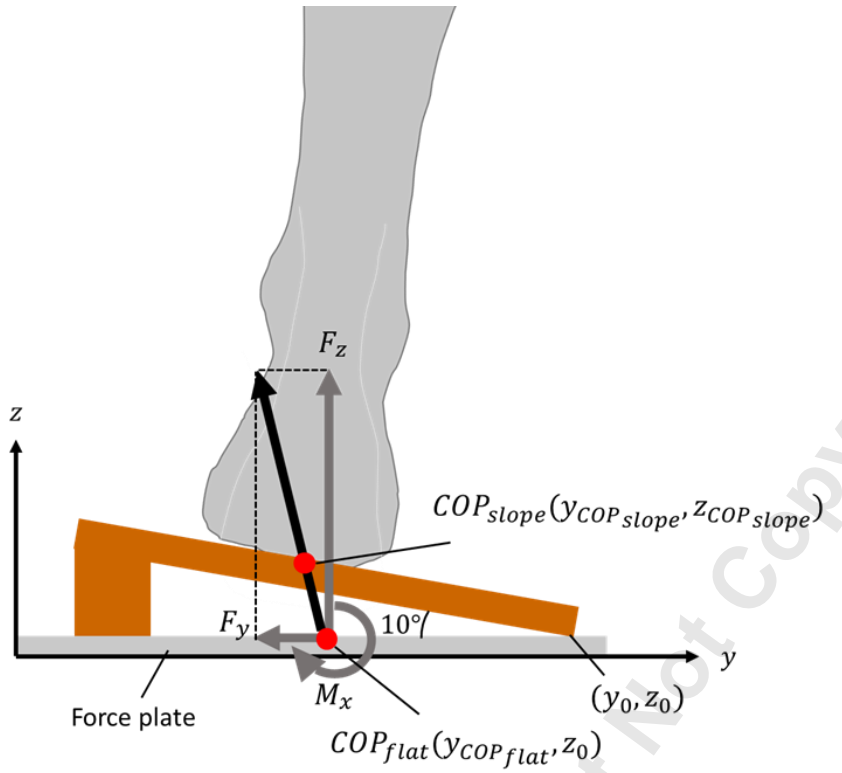

ASME Journal of Engineering and Science in Medical Diagnostics and Therapy. Received February 28, 2022;
Accepted manuscript posted July 22, 2022. doi:10.1115/1.4055040

Fig. 9

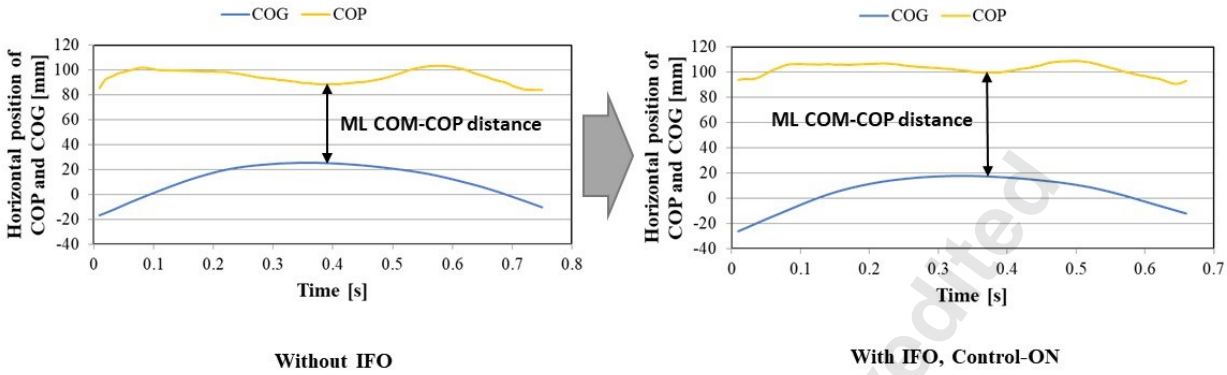

ASME Journal of Engineering and Science in Medical Diagnostics and Therapy. Received February 28, 2022;
Accepted manuscript posted July 22, 2022. doi:10.1115/1.4055040

Fig. 10

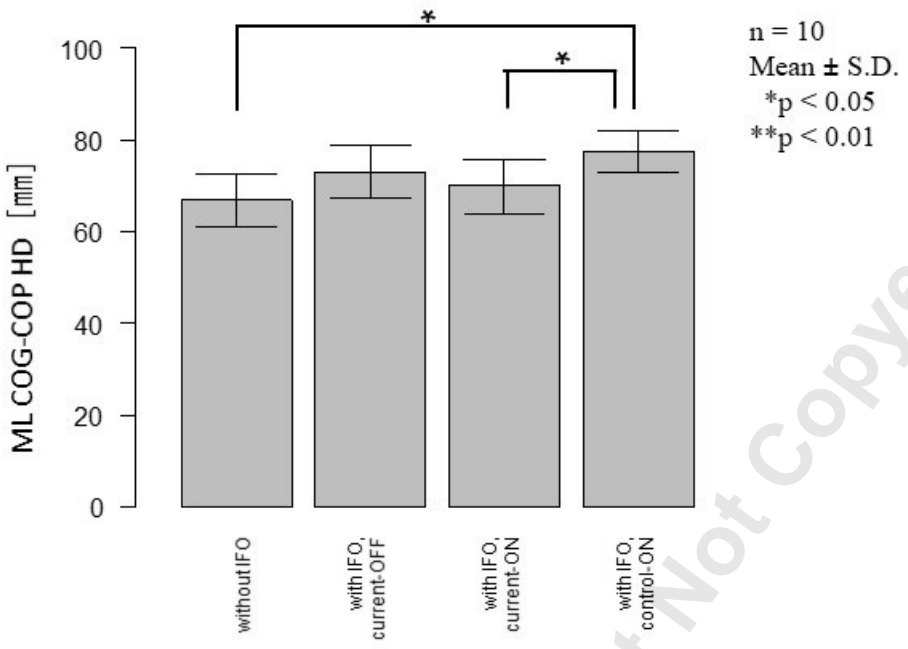

ASME Journal of Engineering and Science in Medical Diagnostics and Therapy. Received February 28, 2022;
Accepted manuscript posted July 22, 2022. doi:10.1115/1.4055040

Fig. 11

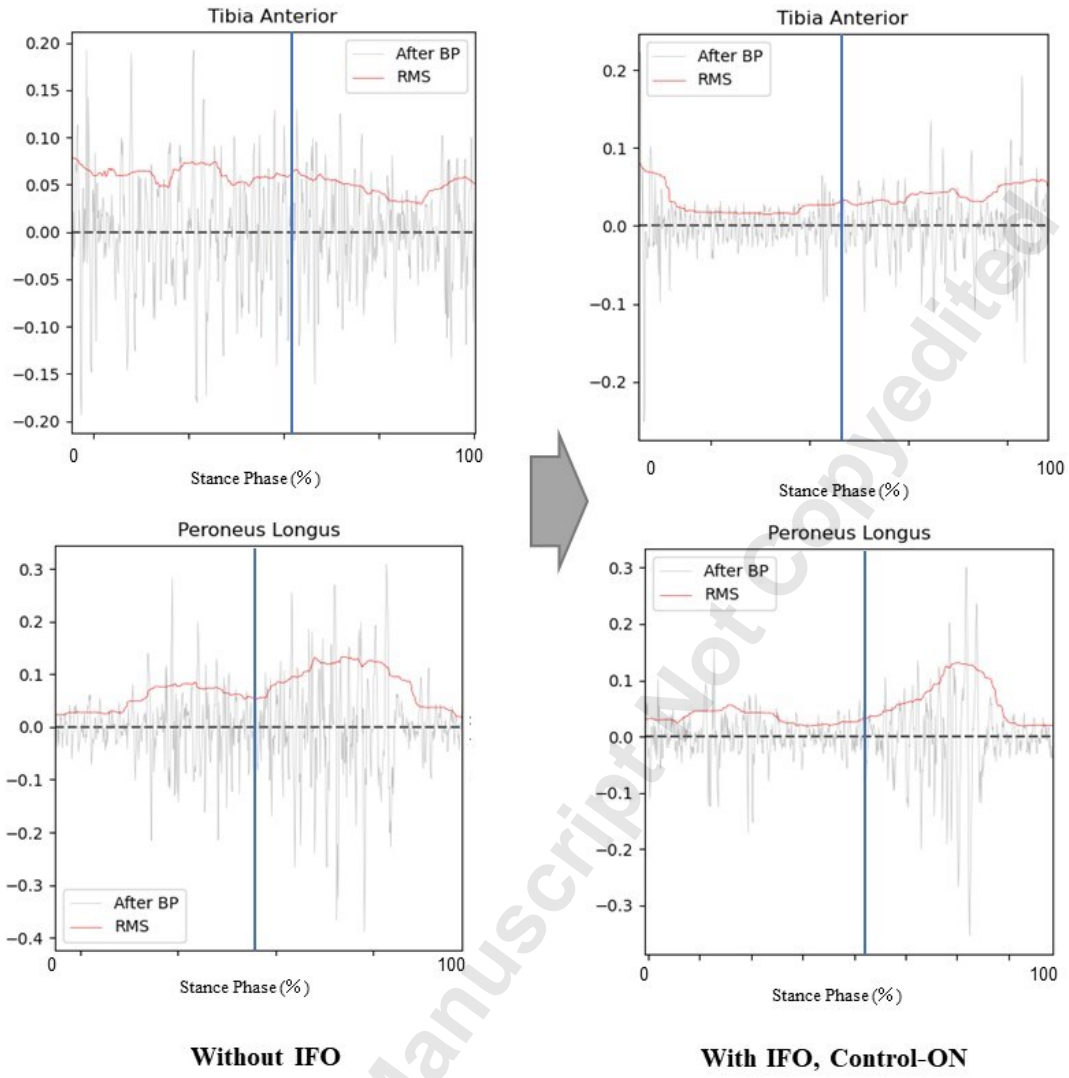

ASME Journal of Engineering and Science in Medical Diagnostics and Therapy. Received February 28, 2022;
Accepted manuscript posted July 22, 2022. doi:10.1115/1.4055040

Fig.12

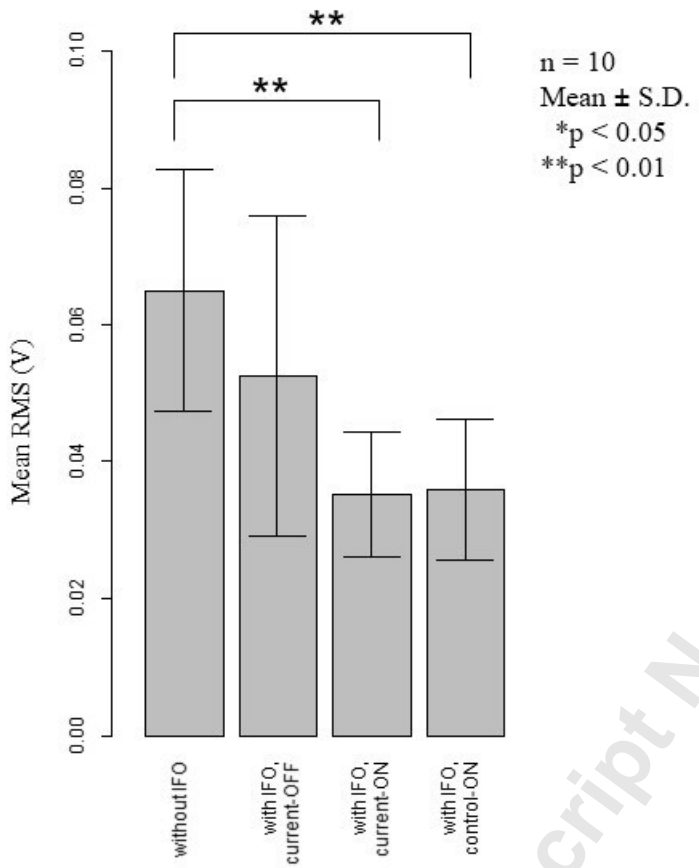

ASME Journal of Engineering and Science in Medical Diagnostics and Therapy. Received February 28, 2022;
Accepted manuscript posted July 22, 2022. doi:10.1115/1.4055040

TABLE CAPTION LIST

Table 1	MR brake Parameters [17]
Table 2	Results summary

ASME Journal of Engineering and Science in Medical Diagnostics and Therapy. Received February 28, 2022;
Accepted manuscript posted July 22, 2022. doi:10.1115/1.4055040

Table 1

MR brake parameters	Value
Mass	128 g
Overall Dimensions	88.4mm×Φ20mm
Maximum generative force	125 N
Maximum current	1.5 A
Maximum voltage	1.3 V
Orifice diameter	0.5 mm
Length of Cylinder	42.4 mm
Cylinder inner diameter	16.5 mm
Piston stroke	7 mm
Piston outer diameter	15.5 mm
Length of piston rod	64.4 mm
Length of piston	12.5 mm
Coil inner diameter	11.5 mm
Number of coil turns	80

ASME Journal of Engineering and Science in Medical Diagnostics and Therapy. Received February 28, 2022;
Accepted manuscript posted July 22, 2022. doi:10.1115/1.4055040

Table 2

Condition	Without IFO	Without IFO	With IFO current-OFF	With IFO current-ON	With IFO control-ON
Type of walkway	Level	Lateral inclined	Lateral inclined	Lateral inclined	Lateral inclined
3D gait analysis					
ML COG–COP HD (mm)	—	66.65 ± 5.69	72.90 ± 5.91	69.81 ± 5.97*	77.40 ± 4.56*†
Surface EMG in the first half of the stance phase					
TA peak (V)	0.040 ± 0.016	0.050 ± 0.017	0.027 ± 0.007	0.034 ± 0.011	0.039 ± 0.008
PL peak (V)	0.064 ± 0.023	0.077 ± 0.024	0.039 ± 0.013*	0.053 ± 0.018	0.057 ± 0.016
Sol peak (V)	0.014 ± 0.006	0.019 ± 0.007	0.010 ± 0.003	0.014 ± 0.006	0.014 ± 0.003
TA mean (V)	0.055 ± 0.024	0.065 ± 0.018	0.053 ± 0.023	0.035 ± 0.009**	0.036 ± 0.010**
PL mean (V)	0.041 ± 0.016	0.050 ± 0.017	0.027 ± 0.007*	0.034 ± 0.011	0.036 ± 0.008
Sol mean (V)	0.020 ± 0.009	0.024 ± 0.005	0.019 ±0.008	0.014 ± 0.004	0.014 ± 0.004

Descriptive statistics are presented as the mean RMS of the EMG ± standard deviation for the variability of all outcomes. The asterisk (*) and double asterisk (**) represent significance levels of *p < 0.05 and **p < 0.01, respectively, compared with the "without IFO" condition. The dagger (†) and double dagger (††) represent significance levels of †p < 0.05 and ††p < 0.01, respectively, compared with the "with IFO current-ON" conditions. EMG: Electromyography, TA: Tibia anterior, PL: Peroneus longus, Sol: Soleus, RMS: Root mean square